Metallic Hydrides II: Materials for Electrochemical Storage

J.-M. Joubert, M. Latroche, and A. Percheron-Guégan

Abstract

For a century, nickel-cadmium (Ni-Cd) batteries have been widely used as electrochemical energy-storage cells. However, due to the rapid development of portable electronic devices and the increasing search for cleaner electric vehicles, new generations of batteries have been investigated during the last few decades. Among them, nickel metal hydride (Ni-MH) batteries, with their larger capacities and improved environmental compatibility, have shown their ability to replace Ni-Cd cells. The negative electrodes of Ni-MH batteries are made of reversibly hydride-forming intermetallic compounds. In this article, the crystallographic and thermodynamic properties of these compounds will be reviewed. Their hydrogen-absorption properties, their electrochemical performance, and the solutions that have been found to achieve reliable cycle life will be presented. The industrial market for Ni-MH batteries will also be discussed in comparison with other battery systems.

Keywords: *aging, alloys, energy-storage materials, hydrogen storage, intermetallic compounds, metallic hydrides.*

Introduction

The exceptional hydrogen-storage properties of $LaNi_5$, which is able to store up to 6.7 hydrogen atoms per formula unit (H/f.u.), were discovered in 1970.[1] Numerous applications were found for this compound and its derivatives, ranging from hydrogen-gas storage to thermal systems such as heat pumps or hydrogen gettering (for a review, see Reference 2). In 1973, Ewe et al. reported the use of this alloy as the negative electrode in an alkali medium,[3] and the first patents for battery applications were filed a few years later.[4] However, the high equilibrium pressure and poor cycle life of $LaNi_5$ make it unusable in practical batteries.[5] In this article, the structural and thermodynamic properties of $LaNi_5$-derived, so-called AB_5 metallic hydrides will be reviewed, and we will show how the equilibrium pressure of the hydride may be adapted to the electrochemical application. Then, the principal causes for degradation will be presented, together with solutions adopted to overcome this problem. Other hydride-forming compounds like AB_2 Laves phases will be briefly described. Finally, the performance of nickel metal hydride (Ni-MH) batteries will be discussed in comparison with other systems.

Structural and Thermodynamic Properties of AB_5 Intermetallic Compounds and Hydrides

Structure of AB_5 and Related Substituted and Nonstoichiometric Compounds

AB_5 intermetallic compounds used for electrochemical applications crystallize in the hexagonal structure described for $LaNi_5$ ($P6/mmm$ space group, $CaCu_5$ structure type) with A(1*a*) in (0,0,0), B(2*c*) in (1/3,2/3,0), and B(3*g*) in (1/2,0,1/2). Both the La and Ni atoms can be substituted with other elements while maintaining the hexagonal $LaNi_5$ parent structure. Lanthanum is easily substituted with other 4*f* elements in the whole range of concentration leading to a complete solid solution for the rare-earth site. Using this property, lanthanum may be easily replaced by misch metal (Mm), a cheaper natural mixing of rare-earth elements.

On the nickel side, a total solid solution in the $LaNi_{5-x}M_x$ system can be attained for some elements like Co, Cu, or Pt, but it is usually limited to a given range of x (e.g., $x \leq 0.6$ for Si, $x \leq 1.2$ for Fe, $x \leq 1.3$ for Al, and $x \leq 2.2$ for Mn).[6] Additionally, the La-Ni phase diagram shows at high temperature a homogeneity domain ranging from $LaNi_{4.85}$ to $LaNi_{5.4}$.[7] The nonstoichiometry in $LaNi_{5+x}$ is interpreted by the presence of randomly distributed nickel-atom pairs (so-called dumbbells), oriented along the *c* axis and replacing lanthanum atoms.[7] Such a structural feature has also been described by Notten et al.[8,9] for ternary copper-substituted alloys. Substitutions and nonstoichiometry may result in drastic changes in the lattice parameters of the intermetallic compound. Owing to the property of binary $LaNi_5$ to melt congruently, single-phase alloys are easily obtained by conventional casting followed by a short annealing treatment.

Structure of Hydrides and the Influence of Substitution

The crystal structure of AB_5 hydrides is studied by means of powder neutron diffraction on deuterated compounds. A huge increase in the lattice parameters accompanies hydrogen insertion, leading to a cell-volume increase of the order of 20% for AB_5H_6. The structure of $LaNi_5D_{6.7}$ was investigated by Lartigue et al.,[10] who observed a deuterium order leading to the doubling of the *c* axis. The consequences of substitution on the structural properties of hydrides have also been widely investigated. It is generally observed that for pseudobinary compounds $LaNi_{5-x}M_x$ (M = Al, Mn, Cu), as well as for the multisubstituted $LaNi_{3.55}Mn_{0.4}Al_{0.3}Co_{0.75}$ of high importance for electrochemical applications, the symmetry and metal-atom positions in the intermetallic compound are preserved upon hydrogenation. Contrary to what is observed for the binary compound, the deuterium is generally not ordered, and the hydride can be described using a structural model involving four partly filled interstitial tetrahedral sites:[11] 4*h* (B_4), 6*m* (A_2B_2), 12*n* (AB_3), and 12*o* (AB_3).

Correlation between Structural and Thermodynamic Properties

Stoichiometric $LaNi_5$ spontaneously reacts with increasing pressures of hydrogen. On the pressure-capacity curve, a pressure plateau (1.7 bar at room temperature) is

observed, corresponding to a phase transition between the hydrogen-poor solid solution in the intermetallic compound (α) and the hydrogen-rich hydride phase (β). $LaNi_5$ is able to store 6.7 H/f.u., but metallic substitutions always lead to a decrease in the hydrogen content, which can be as low as 3.6 H/f.u. for $LaNi_4Cr$.[12] Substitutions either on the nickel or on the lanthanum sublattices involve both a reduction in the storage capacity and a change in the equilibrium pressure. Several groups[13,14] have shown that a linear relation exists between the intermetallic-compound cell volume and the logarithm of the plateau pressure. As the cell volume can be greatly changed by substitutions, this property allows the plateau pressure of the compound to be adapted according to the needs of the electrochemical application by substituting a proper amount of nickel with other elements like Al or Mn. For adequate use, intermetallic compounds for electrochemical applications should be designed with an equilibrium pressure between 0.01 bar and 1 bar at room temperature. Above this pressure range, evolving H_2 gas will compete with electrochemical charging; below this pressure range, poor reversibility and corrosion of the metallic species are likely to occur. Other models allow prediction of the hydride stability, such as those based on thermodynamic[15,16] or electronic properties.[17]

Correlations between structural data and capacity are not as obvious. Some rules have been proposed in order to predict the capacity of metallic hydrides. According to Westlake,[18] a tetrahedron hole size must be larger than 0.4 Å in radius in order to be occupied. Moreover, due to electrostatic repulsion, two neighboring sites cannot be occupied at the same time if their relative distance is less than 2.1 Å.[19] However, these two criteria do not allow the capacity of a pseudobinary compound to be accurately predicted, and a reliable model based on electronic calculations is still missing.

AB_5 Compounds as Electrode Materials

The formation of hydride is commonly obtained by the gas–solid reaction, but it can also be achieved electrochemically in an alkaline electrolyte:

$$MH_x + (y - x)H_2O + (y - x)e^- \rightleftharpoons MH_y + (y - x)OH^-, (E^0 \sim -0.8\ V). \quad (1)$$

Reaction 1 corresponds to the reduction of water and involves one electron per absorbed hydrogen atom. Both the gas–solid and the electrochemical reactions are equivalent: the hydrogen pressure governs the gas–solid process, whereas the equilibrium potential rules the electrochemical reaction. The reversible electrochemical capacity can be related to the quantity of hydrogen absorbed by the gas–solid reaction. Typical values for electrochemical capacities are in the range of 300–320 mAh/g.

Due to the absence of any dense corrosion layer formed after exposure to air, the activation of AB_5 compounds is relatively easy. A typical galvanostatic charge–discharge cycle is shown in Figure 1. For the charge, after a rapidly decreasing branch corresponding to the α domain, the potential shows a plateau corresponding to the progressive transformation from the α phase to the β phase. After 10 h of charge, which corresponds to a full state of charge at 30 mA/g, a small inflection point is observed, and an additional plateau at lower potential appears. It is attributed to the H_2 gas evolving at the surface of the electrode during overcharge. This behavior shows the limit of the electrochemical charging that is counterbalanced by gas evolving when the equivalent equilibrium pressure is above 1 bar. The discharge up to a potential of 300 mV versus a $Cd/Cd(OH)_2$ reference electrode takes place through a highly sloped (rather than a perfectly flat) plateau, leading to about 90% of reversible capacity under the given conditions.

Decrepitation is a degradation phenomenon related to hydrogen insertion–deinsertion, resulting in embrittlement, cracking, and reduction of the particle size. Typical particle sizes of around 10 μm are frequently encountered after hydrogen-gas cycling. In Figure 2a, one can observe the cracking that may result in particles of this size after further cycling. The advantage, in regard to electrochemical applications, is the improvement in the kinetics during cycling due to the increase in the active surface area. However, corrosion is also activated by the renewal of fresh surfaces. Another major drawback is the loss of electrochemical activity in the grains, which is related to the loss of electrical contact due to decohesion of the active material from the electrode.

Bulk oxidation in the corrosive environment of the electrolyte (concentrated KOH) is the most relevant phenomenon responsible for the capacity decrease of AB_5-type materials when used as electrode materials. Pioneering work by Willems[20] has developed all of the basic concepts concerning the corrosion of hydride materials. It was shown that electrochemical-capacity decay results from the decomposition of the intermetallic compound into rare-earth hydroxide and metallic 3*d* elements. More recently, the nature of the corrosion products has been particularly well described by Maurel et al.[21] The characterization was done by simultaneously using x-ray diffraction, scanning electron microscopy, and transmission electron microscopy. The prolonged electrochemical cycling leads to the formation of rare-earth hydroxide needles (see Figure 2b) covering a continuous nanocrystalline corrosion layer composed of metallic (Ni, Co) solid solution

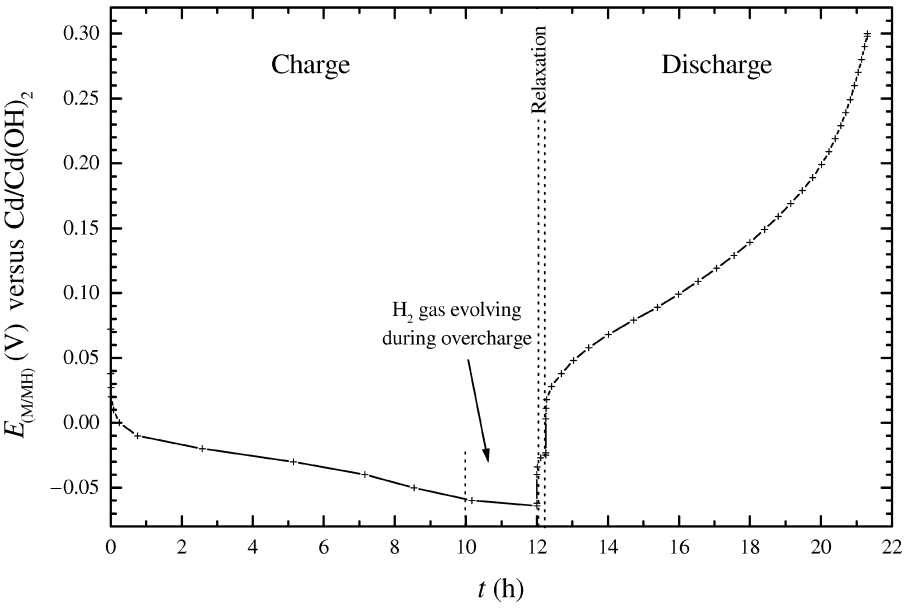

Figure 1. Typical galvanostatic charge–discharge cycle at 30 mA/g for a negative M/MH_x electrode studied in half-cell in 8N KOH electrolyte.

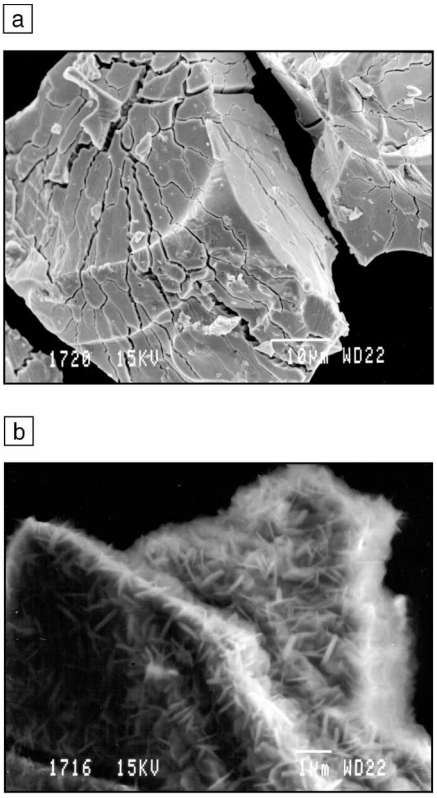

Figure 2. Two manifestations of degradation: (a) decrepitation of $LaNi_{3.55}Mn_{0.4}Al_{0.3}Co_{0.75}$ alloy after 15 hydrogen-gas absorption–desorption cycles, resulting in embrittlement, cracking, and finally reduction of the particle size; (b) rare-earth hydroxide needles resulting from severe corrosion of the same alloy soaked for 8 days in concentrated KOH.

mixed with oxide (Ni, Co)O solid solution and rare-earth hydroxide. This layer itself covers a rare-earth-depleted alloy sublayer.

The main parameter responsible for the corrosion of AB_5-type compounds is related to the presence of rare-earth atoms. As is well known, lanthanides are high-stability hydride-forming elements, but they are also highly oxidizing. Therefore, the relatively poor stability of metallic hydride-forming compounds seems to derive directly from their intrinsic nature to absorb hydrogen. A question of interest is whether the corrosion is due to the immersion in the electrolyte, or to the effect of cycling itself. By analyzing the order of the reaction involving the capacity decay, Willems has shown that the degradation rate is proportional to the actual capacity and, therefore, to the quantity of remaining active material, despite the increase in the surface area induced by the decrepitation phenomenon.[20] In addition, electrodes immersed for prolonged times without cycling did not show any capacity decay. Both observations lead to the conclusion that the corrosion is not related to the time of immersion in the electrolyte (so-called calendar corrosion), but rather to the cycling process itself. Contrary to this finding, Maurel et al.[21] observed the corrosion products of both cycled and noncycled KOH-soaked electrodes and showed that the corrosion products were identical. From these observations, they concluded that the effect of cycling on calendar corrosion was negligible. On the other hand, Merzouki et al.[22] have studied $LaNi_5$ and various substituted derivatives by means of a new technique: the cavity microelectrode. In this technique, micrograms of a sample material are placed in a microcavity at the end of a thin platinum or gold wire embedded in a glass rod. The cavity microelectrode makes it possible to work on very small quantities of material, which thus allows voltametric cycling at very high rates of up to ~100 mV/s. Thousands of cycles may be performed in one day, resulting in negligible calendar corrosion; the observed capacity decrease can be attributed exclusively to the cycling effect. The cycle lives observed are one order of magnitude higher than those measured with conventional cycling methods, which also proves that the calendar effect is dominant in battery applications.

Another cause of degradation seems to be related to the lattice expansion of the compound due to hydrogen insertion during the hydrogenation process. Volume expansion promotes the decrepitation of the alloy, and the resulting increased surface area can corrode. Moreover, as pointed out by Willems,[20] the process of volume expansion itself can result in increased mobility of the rare-earth atoms toward the surface, thereby enhancing the corrosion rate. This conclusion led to the postulation that a reduced lattice expansion should result in more stable (i.e., corrosion-resistant) materials. However, Notten et al.[8,9] have shown that the relevant parameter is not the total lattice expansion, but rather the discrete lattice expansion occurring at the phase transition between saturated α and undersaturated β phases.

Since the early work of Willems,[20] it has been known that substitution could improve chemical resistance to corrosion. Lanthanum replacement by misch metal, in addition to reducing cost, leads to a substantial increase in the electrode cycle life because of the presence of cerium,[23] possibly due to a valence-change effect for this element.[24,25] Cobalt substitution with nickel has also been shown to significantly affect corrosion resistance,[12,23] especially when combined in so-called three-substituted compounds like $MmNi_{3.55}Mn_{0.4}Al_{0.3}Co_{0.75}$,[26] for which synergistic effects between the elements are observed.

In addition to the chemical protection brought about by several substituting elements, another reason for the cycle-life improvement is the reduction in the discrete lattice expansion. Once again, cobalt plays the key role; similar to what occurs in the $LaNi_4Co$-H system,[27] a hydride of composition $LaNi_{3.55}Mn_{0.4}Al_{0.3}Co_{0.75}H_{3.4}$[28] is observed in the lanthanum-based three-substituted compound. The difference is that a second hydride phase is not formed, contrary to what occurs in the $LaNi_4Co$-H system. Instead, an extended solubility branch is observed, in which a large amount of hydrogen can be stored without any lattice discontinuity. This particular feature has been proposed to explain the long-term stability of such a compound[29] because if the electrode is only cycled to ~50% of its full capacity (i.e., mainly cycled in the β branch), energy can be recovered without any phase transition. The resulting discrete lattice expansions are illustrated in Figure 3.

Finally, another possibility for composition modifications has been found by changing the B/A ratio. As shown by Notten et al., the homogeneity domain existing for $LaNi_{5+x}$ can be extended toward the nonstoichiometric (B-rich) region for ternary compounds with Cu[8,9] or Mn.[30] In addition to the diminution in the rare-earth component in these alloys, which can partially explain a less oxidizing character, a strong diminution in the discrete lattice expansion has been observed as a function of the B/A ratio (a discrete lattice expansion as small as 2.8% is observed for $LaNi_{4.4}Cu$). As a result, an improved cycle life has been demonstrated for all of the nonstoichiometric compounds.

In situ neutron diffraction during electrochemical cycling has provided substantial information about the intricate processes taking place in a Ni-MH battery. Due to the highly penetrating power of neutrons, this technique allows operation in geometries very close to industrial batteries in order to follow charge and discharge processes and the nature, quantity, lattice parameters, and deuterium content of the phases involved. One of the most striking features characterized by this technique has been the coexistence of three different phases with compositions 0.5 H/f.u., 3.5 H/f.u., and 5 H/f.u.[31] during the charge of several hydride materials. Again, the presence of the three phases in an out-of-equilibrium state is thought to help in releasing the strains and to play a key role in the corrosion-resistance of the materials.

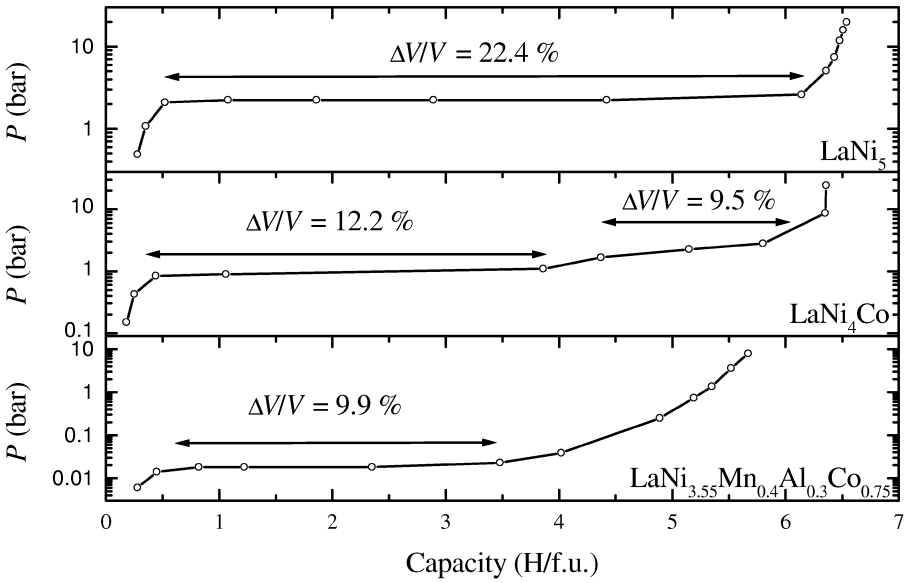

Figure 3. Pressure–composition curves at 25°C for $LaNi_5$, $LaNi_4Co$, and $LaNi_{3.55}Mn_{0.4}Al_{0.3}Co_{0.75}$, showing how the strong discrete lattice expansion, ΔV/V, observed in $LaNi_5$ is split into two parts in the case of $LaNi_4Co$, due to the formation of two hydride phases. The absence of precipitation of the second hydride phase when Mn and Al are substituted together with Co leaves only the precipitation of the first hydride, resulting in a strongly reduced discrete lattice expansion.

Finally, as most of the degradation seems to occur at the surface of the material, various surface modifications have been investigated in order to limit the corrosion. Highly catalytic species at the interface between the electrode and the electrolyte may significantly enhance the dissociation reaction.[32] A hot alkaline treatment seems to be effective in increasing cycle life.[33] However, the reason for this is not clear. On the other hand, fluorination treatment is effective in improving the durability of the electrodes by forming a protective fluoride surface.[34,35] Protective coatings or the use of microencapsulation can also improve cycle life.[36,37]

AB_2 Compounds as an Alternative to AB_5

Due to their larger weight storage density, so-called AB_2 compounds have recently been explored as novel battery materials (for a review, see Reference 38). These compounds are Laves phases crystallizing in either the *C*14 or *C*15 structure types. They are substitutional derivatives of binary compounds made of A = (Zr, Ti) and B = (V, Cr, Mn). These compounds are able to accept substitution on A or B sublattices, particularly with Ni, which allows, as is the case for AB_5 compounds, the plateau pressure to be adapted to electrochemical applications. The electrochemical capacity may reach 400 mAh/g, which represents a gain of nearly 30% as compared with AB_5 compounds. The main problems of these compounds are their poor activation and surface passivation due to a dense corrosion layer inhibiting the charge transfer, and their high corrosion rate due mainly to the high surface area developed during decrepitation. In spite of strong efforts in surface treatment, AB_2 compounds are far from reaching industrial application, although some authors claim the contrary.[39]

Ni-MH Battery Applications

In commercial batteries, agglomerated powders of AB_5 alloys constitute the negative electrode. A small quantity of concentrated KOH is used as the electrolyte, and the positive electrode is the conventional $NiOOH/Ni(OH)_2$ ($E^0 = +0.49$ V) electrode. The whole is packed in tightly sealed cells. The global reaction during charge for one hydrogen atom inserted per metal atom can be written as

$$Ni(OH)_2 + M \rightarrow NiOOH + MH. \quad (2)$$

The reverse is obtained during discharge, giving rise to a voltage of ~1.3 V.

At the end of the charge, gas may evolve, leading to a dramatic increase in pressure inside the tightly sealed cell. To overcome this problem, a recombination process is implemented in the battery: the negative electrode is overcapacitive, in order to prevent any hydrogen-gas formation. Thus, at the end of the charge, oxygen is produced first at the positive electrode following the equation

$$2OH^- \rightarrow H_2O + \frac{1}{2}O_2 + 2e^-. \quad (3)$$

At the negative electrode, the charge will continue:

$$MH_x + 2H_2O + 2e^- \rightarrow MH_{x+2} + 2OH^-. \quad (4)$$

The oxygen gas produced by Reaction 3 flows toward the negative electrode, where recombination takes place by

$$\frac{1}{2}O_2 + MH_{x+2} \rightarrow MH_x + H_2O. \quad (5)$$

Finally, positive- and negative-electrode charge states, gas amount, and water concentration remain constant, preventing any pressure increase or electrolyte drying. However, corrosion of the hydriding alloy leads to irreversible water consumption, and the resulting drying of the separator may limit the cycle life of the battery.

Keeping the same electrolyte and positive electrode makes the replacement of the toxic cadmium negative electrode by metallic hydrides with the same voltage very easy to achieve from an industrial point of view. Besides cycle life and power density, a lot of effort has been directed toward decreasing the cost of these alloys. As mentioned earlier, one way to reduce the cost is to replace pure lanthanum with misch metal, which is about ten times cheaper. However, the alloys remain expensive, essentially because of cobalt, which, while representing only 10% of the alloy weight, may represent up to 40% of its price. Accordingly, several studies have been aimed at reducing the cobalt amount. Substantial reductions have been achieved by preparing nonstoichiometric alloys with only 5 wt% Co. However, despite these efforts, cobalt remains a key element in terms of cycle life for practical alloys.

Table I compares the performance of different battery families. Nowadays, most of the negative electrodes found in commercial Ni-MH batteries are made from AB_5-type materials. The energy densities of actual Ni-MH batteries exhibit values much larger than Ni-Cd ones. The gain reaches 20–30% in terms of weight energy and is about 90% in volume energy (Figure 4). Despite the fact that some efforts are still needed to improve the cycle life (which now reaches 1000 cycles) and kinetics and to decrease the cost of Ni-MH batteries, they are already superior to Ni-Cd batteries in terms of energy density

Table I: Comparisons of Different Battery Families.

	Ni-Cd	Ni-MH	Li-Ion
Voltage (V)	1.28	1.3	3.8
Weight Energy (Wh/kg)	45–55	60–75	120–160
Volume Energy (Wh/dm^3)	80–150	220–300	200–350
Power (W/kg)	400–600	1000	1350
Cycle Life (number of cycles)	2000	1000	1500
Pollution Concerns	Cd toxicity	No major toxicity	No major toxicity
Cost (USD/kWh)	$297	$327	$808

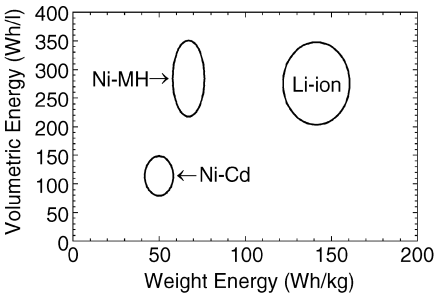

Figure 4. Energy by volume as a function of energy by weight for different battery systems.

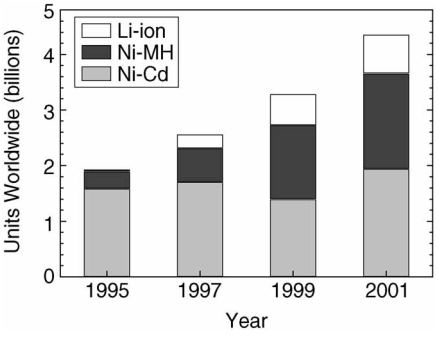

Figure 5. Market evolution of various battery systems.

and environmental impact. Li-ion batteries are nowadays the most serious competitor for Ni-MH batteries, mainly due to their higher weight energy (see the August 2002 issue of *MRS Bulletin*). However, Li-ion batteries are expensive and require a long charging time. Actually, it seems that the choice among the different battery families in portable equipment depends mainly on the application. For instance, Ni-Cd batteries are very efficient for portable tools, Ni-MH batteries dominate in cellular phones, and Li-ion batteries are preferred in laptop computers. Today, the production of batteries is in the billions of units worldwide, and the market is shared approximately equally between Ni-Cd and Ni-MH, as can be seen in Figure 5.

Ni-MH cylindrical cells are designed for telecommunications and other portable applications. The latest generation of Ni-MH batteries target applications requiring fast charge and discharge rates (e.g., cordless power tools, electric bikes, personal electric vehicles, radio-controlled models, portable medical equipment). As an example, Saft Batteries has recently announced that it will be the supplier of self-contained batteries for the Segway Human Transporter, the first dynamical self-balancing, electric-powered transportation machine. There are also several electric vehicle projects in which Ni-MH batteries are used. Toyota has recently developed a new car concept, the Prius, which is powered by both an internal-combustion engine and an advanced electric motor. Depending on the driving conditions, one or both are used to maximize fuel efficiency and minimize emissions. The car never needs to be plugged in because the engine recharges the batteries automatically. The Prius compact lightweight battery pack comprises 38 sealed Ni-MH modules, designed to be charged tens of thousands of times without any external power source.

References

1. J.H.N. Van Vucht, F.A. Kuijpers, and H.C.A.M. Bruning, *Philips Res. Rep.* **25** (1970) p. 133.
2. L. Schlapbach, in *Hydrogen in Intermetallic Compounds II: Topics in Applied Physics,* Vol. 67, edited by L. Schlapbach (Springer, Berlin, 1992) p. 328.
3. H.H. Ewe, E.W. Justi, and K. Stephan, *Energy Conversion* **13** (1973) p. 109.
4. F.G. Will, U.S. Patent No. 3,874,958 (1975).
5. H.F. Bittner and C.C. Badcock, *J. Electrochem. Soc.* **130** (1983) p. 193C.
6. A. Percheron-Guégan, C. Lartigue, and J.-C. Achard, *J. Less-Common Met.* **109** (1985) p. 287.
7. K.H.J. Buschow and H.H. van Mal, *J. Less-Common Met.* **29** (1972) p. 203.
8. P.H.L. Notten, R.E.F. Einerhand, and J.L.C. Daams, *J. Alloys Compd.* **210** (1994) p. 221.
9. P.H.L. Notten, J.L.C. Daams, and R.E.F. Einerhand, *J. Alloys Compd.* **210** (1994) p. 233.
10. C. Lartigue, A. Percheron-Guégan, J.-C. Achard, and J.-L. Soubeyroux, *J. Less-Common Met.* **113** (1985) p. 127.
11. A. Percheron-Guégan and C. Lartigue, *Mater. Sci. Forum* **31** (1988) p. 125.
12. T. Sakai, K. Oguro, H. Miyamura, N. Kuriyama, A. Kato, and H. Ishikawa, *J. Less-Common Met.* **161** (1990) p. 193.
13. J.-C. Achard, A. Percheron-Guégan, H. Diaz, F. Briaucourt, and F. Demany, in *Proc. 2nd Int. Congress on Hydrogen in Metals* (Pergamon Press, Oxford, 1977) p. 1E12.
14. M.H. Mendelsohn, D.M. Gruen, and A.E. Dwight, *Nature* **269** (1977) p. 45.
15. A.R. Miedema, *J. Less-Common Met.* **32** (1973) p. 117.
16. A.R. Miedema, R. Boom, and F.R. de Boer, *J. Less-Common Met.* **41** (1975) p. 283.
17. R. Griessen and A. Driessen, *Phys. Rev. B* **30** (8) (1984) p. 4372.
18. D.G. Westlake, *J. Less-Common Met.* **90** (1983) p. 251.
19. A.C. Switendick, *Z. Phys. Chem. NF* **117** (1979) p. 89.
20. J.J.G. Willems, *Suppl. Philips J. Res.* **39** (1984) (Suppl. 1) p. 1.
21. F. Maurel, B. Knosp, and M. Backhaus-Ricoult, *J. Electrochem. Soc.* **147** (1) (2000) p. 78.
22. A. Merzouki, C. Cachet-Vivier, V. Vivier, J.-Y. Nédélec, L.T. Yu, N. Haddaoui, J.-M. Joubert, and A. Percheron-Guégan, *J. Power Sources* **109** (2002) p. 281.
23. J.J. Reilly, G.D. Adzic, J.R. Johnson, T. Vogt, S. Mukerjee, and J. McBreen, *J. Alloys Compd.* **293–295** (1999) p. 569.
24. S. Mukerjee, J. McBreen, J.J. Reilly, J.R. Johnson, G. Adzic, K. Petrov, M.P.S. Kumar, W. Zhang, and S. Srinivasan, *J. Electrochem. Soc.* **142** (7) (1995) p. 2278.
25. V. Paul-Boncour, J.-M. Joubert, M. Latroche, and A. Percheron-Guégan, *J. Alloys Compd.* **330–332** (2002) p. 246.
26. H. Ogawa, M. Ikoma, H. Kawano, and I. Matsumoto, *J. Power Sources* **12** (1988) p. 393.
27. D. Chartouni and K. Gross, *J. Electrochem. Soc.* **148** (3) (2001) p. A241.
28. M. Latroche, A. Percheron-Guégan, and F. Bourée-Vigneron, *J. Alloys Compd.* **265** (1–2) (1998) p. 209.
29. M. Latroche, A. Percheron-Guégan, Y. Chabre, J. Bouet, J. Pannetier, and E. Ressouche, *J. Alloys Compd.* **231** (1995) p. 537.
30. P.H.L. Notten, M. Latroche, and A. Percheron-Guégan, *J. Electrochem. Soc.* **146** (1999) p. 3181.
31. M. Latroche, Y. Chabre, A. Percheron-Guégan, O. Isnard, and B. Knosp, *J. Alloys Compd.* **330–332** (2002) p. 787.
32. P.H.L. Notten and P. Hokkeling, *J. Electrochem. Soc.* **138** (7) (1991) p. 1877.
33. M. Ikoma, K. Komori, S. Kaida, and C. Iwakura, *J. Alloys Compd.* **284** (1999) p. 92.
34. M. Sakashita, Z.P. Li, and S. Suda, *J. Alloys Compd.* **253-254** (1997) p. 500.
35. Y.-M. Sun, K. Ywata, S. Chiba, Y. Matsuyama, and S. Suda, *J. Alloys Compd.* **253–254** (1997) p. 520.
36. M. Geng, *J. Alloys Compd.* **206** (1994) p. L3.
37. T. Sakai, A. Yuasa, H. Ishikawa, H. Miyamura, and N. Kuriyama, *J. Less-Common Met.* **172–174** (1991) p. 1194.
38. F. Cuevas, J.-M. Joubert, M. Latroche, and A. Percheron-Guégan, *Appl. Phys. A* **72** (2001) p. 225.
39. S.R. Ovshinsky, M.A. Fetchenko, and J. Ross, *Science* **260** (1993) p. 176. □